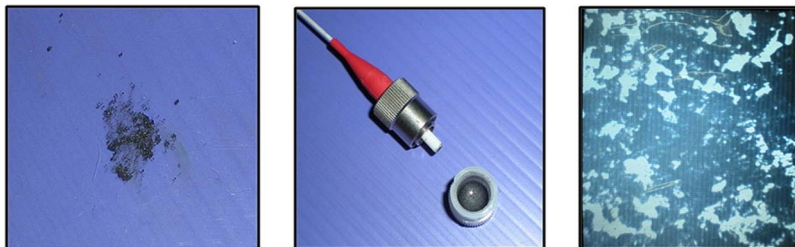


2.0- μm Q-Switched Thulium-Doped Fiber Laser With Graphene Oxide Saturable Absorber

Volume 5, Number 4, August 2013

H. Ahmad
A. Z. Zulkifli
K. Thambiratnam, Member, IEEE
S. W. Harun



DOI: 10.1109/JPHOT.2013.2273733
1943-0655/\$31.00 ©2013 IEEE

2.0- μm Q-Switched Thulium-Doped Fiber Laser With Graphene Oxide Saturable Absorber

H. Ahmad, A. Z. Zulkifli, K. Thambiratnam, *Member, IEEE*, and S. W. Harun

Photonics Research Centre, University of Malaya, 50603 Kuala Lumpur, Malaysia

DOI: 10.1109/JPHOT.2013.2273733
1943-0655/\$31.00 © 2013 IEEE

Manuscript received May 25, 2013; revised July 11, 2013; accepted July 13, 2013. Date of publication July 17, 2013; date of current version July 26, 2013. This work was supported by the University of Malaya under Grants UM.C/625/1/HIR/MOHE/SCI/29, MOHE, RG143-12AET, and RU002-2013. Corresponding author: H. Ahmad (e-mail: harith@um.edu.my).

Abstract: A compact Q-switched thulium-doped fiber laser (TDFL) operating near the 2.0- μm region is proposed and demonstrated. The proposed laser uses a 2-m-long thulium-doped fiber with a core absorption of 27 dB/m at 793 nm as the active medium and a graphene oxide (GO)-based saturable absorber (SA) as the Q-switching element. The SA is fabricated by optically depositing GO particles dissolved in distilled water onto the face of a fiber ferrule, which is then used to assemble the SA. The proposed TDFL is capable of generating pulses with a maximum repetition rate of 16.0 kHz and pulsewidths as narrow as 9.8 μs , as well as having maximum average output power and pulse energy of 0.3 mW and 18.8 nJ, respectively. The combination of the easily fabricated GO-based SA, together with the TDFL's ability to operate in the eye-safe region of 2.0 μm , gives the proposed Q-switched TDFL a high potential for a multitude of real-world applications, including range-finding, medicine, and spectroscopy.

Index Terms: Q-switch, thulium-doped fiber, 2 μm fiber laser, graphene oxide, saturable absorber.

1. Introduction

Thulium doped fibers (TDFs), operating in the 1.85 to 2.0 μm wavelength band, have become the focus of intense research efforts due to their significant potential in a multitude of applications such as in medicine, manufacturing and high resolution spectroscopy [1], [2]. Passively Q-switched TDF lasers (TDFLs) are particularly desirable for use in a variety of 'eye-safe' applications such as laser range-finders, coherent Doppler wind light detection and ranging (LIDAR) and differential absorption LIDAR systems [3]–[7], where the pulses need not be very short. Q-switched TDFLs also have the advantage of generating outputs with higher pulse energies [8], and do not require the delicate balancing of losses traditionally associated with mode-locking, thereby increasing the operational efficiency and reducing the complexity of the system.

Q-switched fiber lasers can be obtained using either active or passive modulation. Active modulation is achieved by the use of an external device, such as an acoustic- or electro-optic modulator, which provides a high degree of control over the generated pulse. This approach however makes the Q-switched fiber laser bulky and expensive, as well as highly fragile and sensitive to environmental influences such as electromagnetic fields and high temperatures. Passive Q-switching on the other hand, using Semiconductor Saturable Absorption Mirrors (SESAMs) [9] or Saturable Absorbers (SAs) [10], allow for more robust, compact and efficient fiber laser systems to be realized.

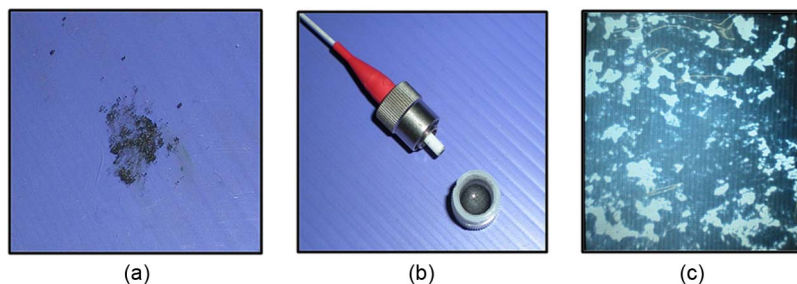


Fig. 1. Images of the GO in two different forms (a) nano-powder, (b) aqueous solution. (c) The optical fiber scope image of the GO-SA on a fiber ferrule face after optical deposition process. The dark areas are the GO layers, while the bright areas are the parts of the fiber ferrule not covered by the GO particles.

Of the two, SAs are typically preferred for generating pulsed outputs due to their compact size as SESAMs tend to be complex and expensive quantum well structures and its fabrication requires molecular beam epitaxy on distributed Bragg reflectors [11], [12]. SAs can take many forms, but of late the allotropes of carbon such as graphene and Carbon Nanotubes (CNTs) have proven themselves to be very capable as SAs for Q-switched lasers [5], [13]. Graphene in particular has seen substantial deployment as an SA due to its remarkable optical properties; graphene based SAs are capable of nonlinear saturable absorption as a result of Pauli blocking with a wide operating spectral range [14], [15]. Recently, Graphene Oxide (GO) has also emerged as a highly viable candidate for SAs. While both graphene and GO share similar mechanical, electronic and optical characteristics; graphene cannot dissolve into water, thus making the graphene SA somewhat difficult to fabricate. GO on the other hand easily dissolves in water, due to the carboxyl and hydroxyl groups in its structure. Furthermore, GO is a precursor for graphene and can therefore be obtained by a very low-cost and simple fabrication method [16].

However, despite the latent capabilities of graphene in generating Q-switched pulses, research into similar TDFL based systems seems to be severely limited. There have only been a few demonstrations of passively Q-switched TDFLs using graphene based SAs, [4], [5], [7] and to the best of the author's knowledge, none using GO based SAs. In this paper, a Q-switched TDFL in a simple ring cavity is proposed and demonstrated, using a 2 m long TDF as the active gain medium and a GO-based SA as the Q-switching element. The proposed TDFL is capable of generating Q-switch pulses with a pulse-width as narrow as $9.8 \mu\text{s}$ and having a maximum repetition rate of 16.0 kHz. This is the first time, to the best knowledge of the authors, that a Q-switched TDFL with a GO based SA is demonstrated.

2. Preparation of the GO Based SA

The GO used in this work is obtained from Graphene Research Ltd. in a dry nano-powder form as shown in Fig. 1(a). The GO is dissolved in distilled water to form an aqueous solution Fig. 1(b) that will be used in the fabrication of the SA. The SA is formed by depositing the GO layer onto the face of the fiber ferrule, based on the optical deposition technique as demonstrated by Kashiwagi *et al.* [17] in the case of CNT, and subsequently demonstrated by Martinez, *et al.* [18] using CNTs and graphene. A similar approach has also recently been shown for the deposition of a layer of GO onto the ferrule of an optical fiber [19], which forms the basis of this work.

In order to form the GO-based SA, one end of a FC/PC fiber patch cord is immersed in the aqueous solution. The other end of the patch cord is connected to an amplified spontaneous emission (ASE) source, operating at 15 dBm. Due to the thermophoresis effect, GO layers are formed on the face of the fiber ferrule after approximately half an hour, upon which the ferrule is removed from the solution and then left to dry for another half an hour. The image of the GO-SA on a fiber ferrule face is observed using the optical fiber scope as shown in Fig. 1(c).

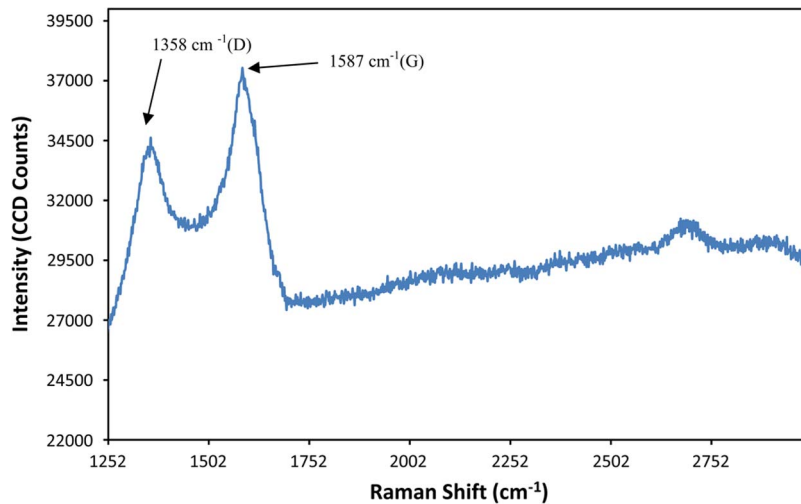


Fig. 2. Raman spectrum of GO on the fiber ferrule face.

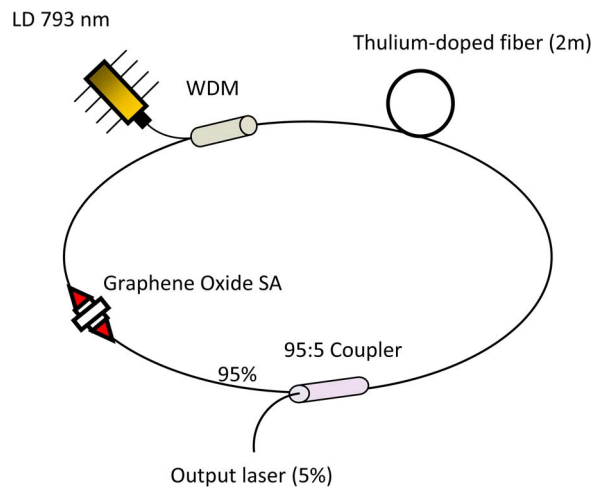


Fig. 3. Setup of the proposed Q-switched TDFL with GO-based SA.

The deposited GO layers are analyzed by Raman spectrometry using a Renishaw Raman Spectrometer to detect any disorder and defects in the material. The obtained spectrum is shown in Fig. 2.

The two main peaks observed in the spectrum, known as the D and G peaks are typical to that of GO, with the D peak observed at 1358 cm^{-1} and the G peak observed at 1587 cm^{-1} [20]–[22]. It is also important to note that there are no peaks in the Raman spectrum at the region of 2700 cm^{-1} , called the 2-D or G' band which would confirm the presence of graphene [23], [24]. Once the spectrometry analysis has been completed and the successful deposition of the GO layers confirmed, the fiber ferrule is then connected to another patch cord using an FC/PC adaptor to complete the assembly of the SA.

3. Experimental Setup for Q-Switched Pulse Generation

The experimental setup of the proposed Q-switched TDFL is shown in Fig. 3. The setup consists of a 2 m long single-mode TDF from Nufern, USA, which has a core absorption of 27.0 dB/m at 793 nm with a cutoff wavelength at 1750 nm and core and cladding diameters of $9\text{ }\mu\text{m}$ and $125\text{ }\mu\text{m}$, respectively.

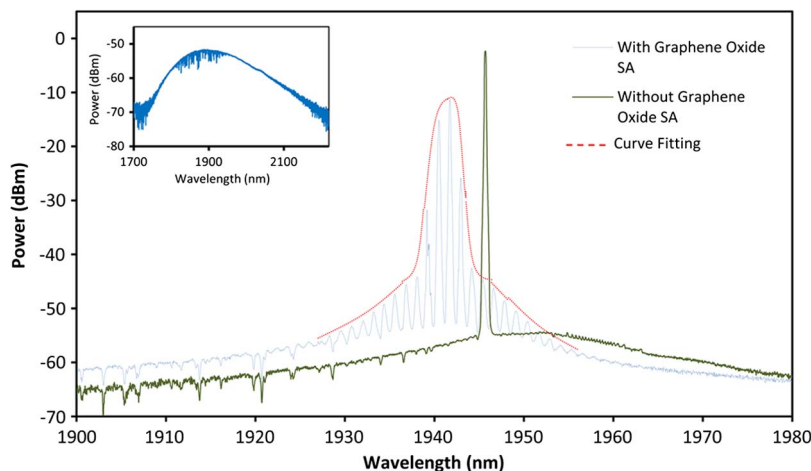


Fig. 4. Thulium-doped fiber laser spectra with and without the GO based SA and a curve fit that envelopes the Q-switched laser spectrum for FWHM measurement. The inset shows the ASE spectrum of the TDF.

The TDF is core-pumped by a single mode Lumics 793M200 laser diode (LD) operating at 793 nm with a maximum output power of 164 mW. The LD pumps the TDF through an 800/2000 nm fused wavelength division multiplexer (WDM), with the LD connected to the 800 nm port. The common port of the WDM is connected to one end of the TDF, while the other end of the TDF is connected to an AC Photonics Inc. 95:5 tap coupler. It must be noted that the tap coupler is designed for use in the 1550 nm region, and this may result in slight losses to the system, although not to the extent that the performance of the system will be severely affected. The 95% port of the tap coupler is connected to the GO-based SA assembly, with the other end of the SA connected to the 2000 nm port of the WDM, thus completing the optical circuit. The 5% port of the tap coupler is used to extract a small portion of the oscillating signal for further analysis.

4. Results and Discussion

The lasing output of the TDFL is shown in Fig. 4, and is obtained from a Yokogawa AQ6375 optical spectrum analyzer (OSA) with a span setting of 515 nm and a resolution setting of 0.2 nm placed at the 5% port of the TDFL setup. The LD is set to operate at 128.8 mW, with the SA initially removed from the optical cavity. Under these conditions, a single lasing wavelength at 1945.0 nm is observed, with a peak power of about -2.6 dBm. The lasing wavelength is well defined, with a signal-to-noise ratio (SNR) of approximately 54 dB and a full width at half maximum (FWHM) bandwidth of 0.2 nm. Inserting the GO-based SA however changes the output of the TDFL, widening the bandwidth to approximately 1.0 nm due to the laser now operating in the Q-switching regime. At the same time, the center wavelength of the laser blue-shifts to 1941.7 nm. The shift is induced as a result of the losses incurred when the SA is integrated into the laser cavity, thereby forcing the system to compensate for these by moving towards the region of higher gain [25]. The losses incurred also lowers the peak power of the system, with the lasing wavelength now having a lower peak power of only -12.0 dBm.

The inset of Fig. 4 shows the ASE spectrum obtained from the TDF when pumped under similar conditions, but without the presence of a seed signal or feedback loop. The ASE spectrum can be seen to stretch from 1760.0 nm to approximately 2118.0 nm, giving a bandwidth of about 5 nm with a peak power of -52 dBm at approximately 1890 nm.

In order to analyze the Q-switched pulses generated by the TDFL, the OSA is removed from the setup, and replaced with an EOT Inc. ET-5010F Indium-Gallium-Arsenide (InGaAs) photodetector connected to a LeCroy oscilloscope with a bandwidth of 500 MHz. The InGaAs photodetector is designed for operation in the $2.0 \mu\text{m}$ region, with a bandwidth from 1475 nm to 2100 nm. Fig. 5(a)

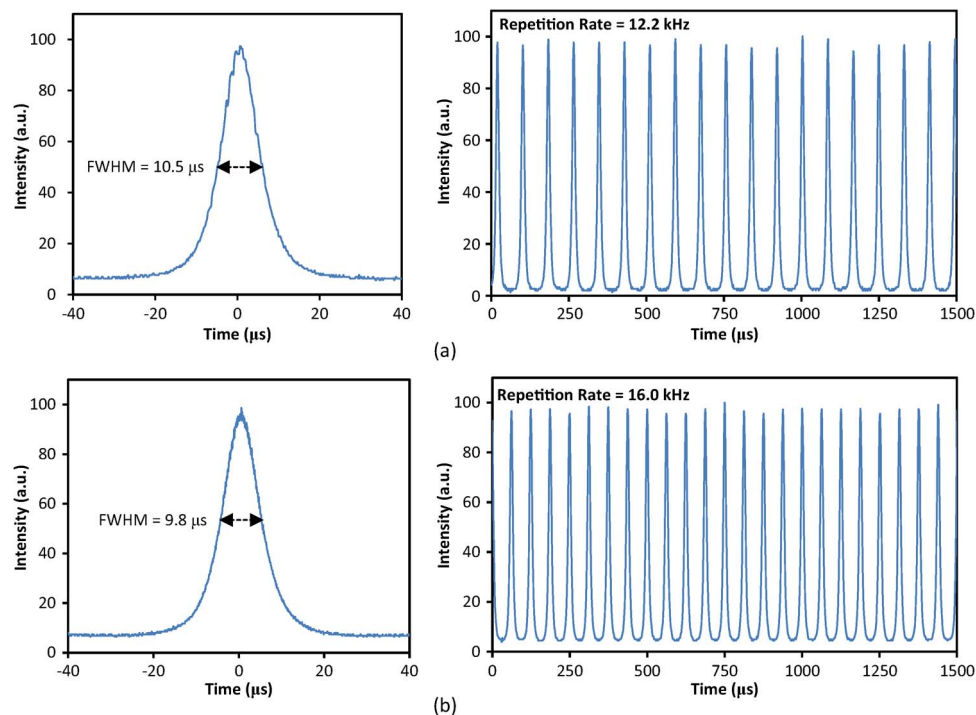


Fig. 5. Single pulse and a pulse train of a Q-switched laser at a pump power of (a) 148 mW and (b) 164 mW. Under a pump power of 148 mW, the intensity of the pulses have a standard deviation of about 1.2426, dropping to 1.2216 at a pump power of 164 mW.

and (b) show the normalized single pulse and pulse train obtained from the TDFL under pump powers of 148 and 164 mW.

The trace of the pulse is better defined at the higher pump power, with the walls of the trace having better continuity and fewer “jagged peaks”. Similarly, the repetition rates of the pulse trains increases as the pump power is raised, from a repetition rate of 12.2 kHz at a pump power of 148 mW to a repetition rate of 16.0 kHz at a pump power of 164 mW. It can also be seen that at higher pump powers, the pulse train is more stable, with fewer peak intensity fluctuations than at lower pump powers. This is further validated by the fact that the profile of the pulse at a higher pump powers is better defined, as compared to the profile obtained at lower pump powers.

Fig. 6 shows the repetition rates and pulse widths of the output pulses against different pump powers. The obtained repetition rate increases as the pump power is raised, with a lasing threshold of about 100 mW and a Q-switching threshold of 125 mW. The response of the repetition rate is linear to the pump power, increasing at an initial slope of 0.3 kHz/mW until a pump power of 144 mW is reached, after which the slope reduces slightly to 0.2 kHz/mW until the maximum pump power of 164 mW is reached. The pulse width on the other hand decreases as the pump power increases, from an initially steep slope of $-0.86 \mu\text{s}/\text{mW}$, before becoming shallower at $-0.24 \mu\text{s}/\text{mW}$ above a pump power of 132.5 mW. At a pump power of about 148.4 mW, increases in the pump power result in only a minor change in the pulse width, with the slope at this region computed to be around $-0.045 \mu\text{s}/\text{mW}$. The slower changes in the pulse width and repetition rate at higher pump powers can be attributed to the GO-SA reaching saturation, and it can be predicted that further increases in the pump power will push the SA closer toward saturation, and result in little to no change in the pulse width or repetition rates, as long as the damage threshold of the SA is not exceeded.

Fig. 7 shows the average output powers and pulse energies obtained as the pump power increases. The output power is measured by a Melles Griot 13PEM001 broadband power meter which is placed at the 5% output port of the TDFL’s cavity. It can be seen from Fig. 7 that the output pulses are typical in behavior to that of Q-switched pulses, with the average output power reaching

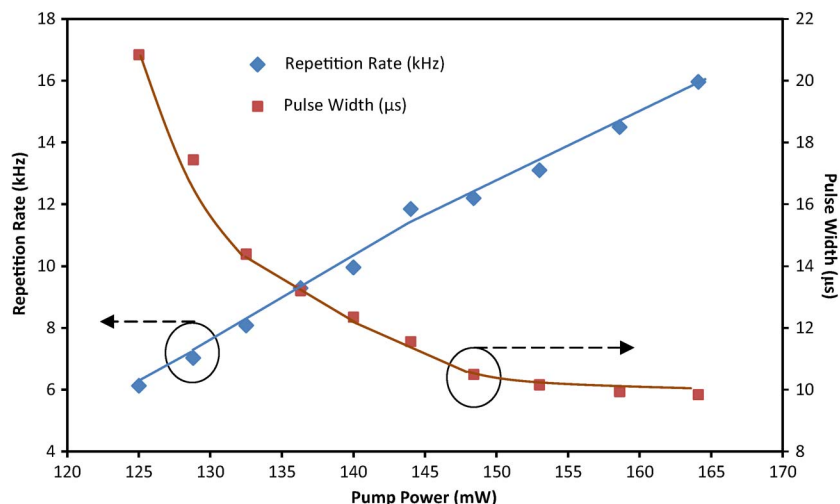


Fig. 6. Repetition rate and pulse width curves as function of pump power.

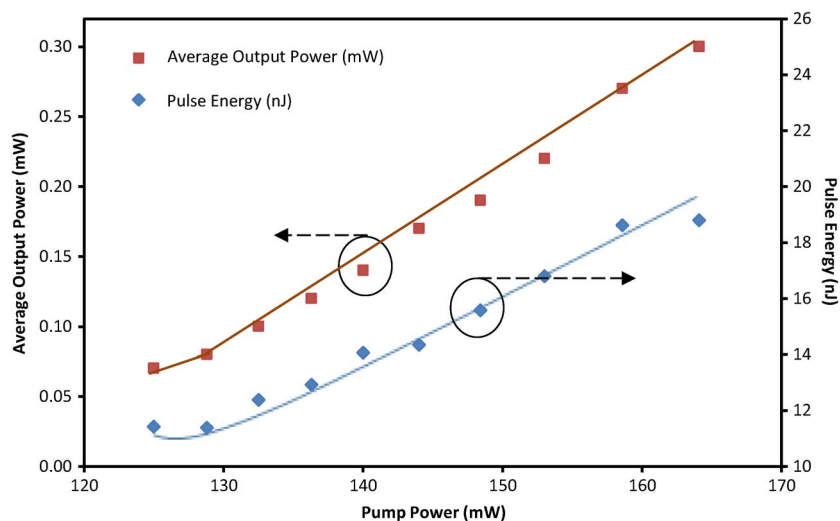


Fig. 7. Average output power and pulse energy curves as function of pump power.

a maximum of 0.3 W at a pump power of 125 mW to a maximum pump power of 164 mW. The increase is almost linear with a slope efficiency of 0.0063, and only minor variations from the fitted line. The pulse energy rises with the repetition rate, increasing from 11.4 nJ at a pump power of around 125 mW, to 18.8 nJ at the maximum pump power of 164 mW, with an average slope of about 0.21 nJ/mW.

The stability of the Q-switched pulse train is analyzed by connecting an Anritsu MS2683A radio frequency spectrum analyzer (RFSA) together with the ET-5010F InGaAs photodetector at the 5% port of the TDFL. The obtained RFSA spectrum, at a resolution and video bandwidth of 300 Hz along a 22 kHz span is shown in Fig. 8.

Fig. 8 shows the fundamental harmonic, occurring at a frequency of 12.2 kHz. The fundamental harmonic has a peak power of approximately -43.0 dBm, giving it a peak-to-floor ratio of about 28.0 dB. The peak-to-floor ratio is higher than the threshold value of 20.0 dB, thus indicating that the output pulses are stable [26]. Furthermore, there is no indication of high frequency harmonics suppression, as indicated by the inset which shows the radio frequency harmonics, including the

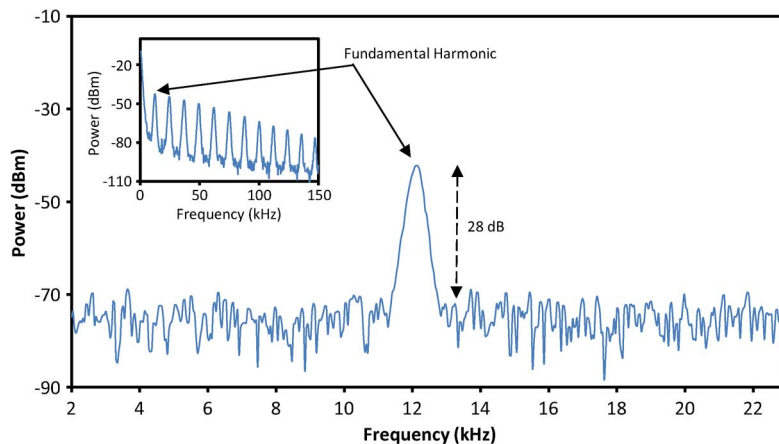


Fig. 8. Radio frequency measurement of Q-switched laser at a repetition rate of 12.2 kHz using RFSA, with inset showing the RF harmonics of the laser pulses.

fundamental harmonic and up to the 12th harmonic. This indicates that the pulses have a short rise and fall time, and augers well with the pulse widths and repetition rates discussed earlier.

The proposed Q-switched TDFL is capable of providing a pulsed laser output at the 2.0 μm region in a compact and easy to operate form factor. The proposed TDFL has numerous applications in range-finding and sensing, and is relatively easy to fabricate. This is the first time, to the knowledge of the authors, that a Q-switched TDFL, operating in the 2.0 μm region, has been demonstrated using a GO-based SA. This is also the first time, to the best knowledge of the authors, that a GO-based SA has been fabricated by optically depositing GO layers on the face of the fiber ferrule.

5. Conclusion

A compact, Q-switched TDFL using a GO-based SA for operation in the 2.0 μm region is demonstrated. The active medium of the proposed pulse laser is a 2 m long TDF with an absorption rate of 27 dB/m at 793 nm. The GO-based SA is fabricated by optically depositing GO particles suspended in an aqueous solution on the face of a fiber ferrule, then sandwiching the deposited GO layer against another fiber ferrule. The Q-switched TDFL is capable of generating pulses with a maximum repetition rate, average output power and pulse energy of 16.0 kHz, 0.3 mW and 18.8 nJ, respectively at a pump power of 164 mW. The pulse widths obtained at this pump power are also the narrowest for the system, at 9.8 μs . The proposed Q-switched TDFL is suitable for a multitude of real-world applications such as range-finding, medicine and spectroscopy due to its ability to operate in the eye-safe region of 2.0 μm .

References

- [1] P. F. Moulton, G. A. Rines, E. V. Slobodtchikov, K. F. Wall, G. Frith, B. Samson, and A. L. G. Carter, "Tm-doped fiber lasers: Fundamentals and power scaling," *IEEE J. Sel. Topics Quantum Electron.*, vol. 15, no. 1, pp. 85–92, Jan./Feb. 2009.
- [2] S. D. Jackson, A. Sabella, and D. G. Lancaster, "Application and development of high-power and highly efficient silica-based fiber lasers operating at 2 μm ," *IEEE J. Sel. Topics Quantum Electron.*, vol. 13, no. 3, pp. 567–572, May/Jun. 2007.
- [3] Y. Tang, C. Huang, S. Wang, H. Li, and J. Xu, "High-power narrow-bandwidth thulium fiber laser with an all-fiber cavity," *Opt. Exp.*, vol. 20, no. 16, pp. 17 539–17 544, Jul. 2012.
- [4] B. Lu, H. Chen, M. Jiang, X. Chen, Z. Ren, and J. Bai, "Graphene-based passive Q-switching for a 2 μm thulium-doped fiber laser," *Laser Phys.*, vol. 23, no. 4, p. 045111, Apr. 2013.
- [5] F. Wang, F. Torrisi, Z. Jiang, D. Popa, T. Hasan, Z. Sun, W. Cho, and A. C. Ferrari, "Graphene passively Q-switched two-micron fiber lasers," presented at the Quantum Electronics Laser Science Conf., San Jose, CA, USA, May 2012, Poster Session I (JW2A).
- [6] Q. Q. Wang, T. Chen, M. Li, B. Zhang, A. P. Heberle, and K. P. Chen, "Passively Q-switched thulium-doped fiber laser by graphene saturable absorber," in *Proc. 17th OECC*, Busan, Korea, 2012, pp. 55–56.
- [7] M. Jiang, H. F. Ma, Z. Y. Ren, X. M. Chen, J. Y. Long, M. Qi, D. Y. Shen, Y. S. Wang, and J. T. Bai, "A graphene Q-switched nanosecond Tm-doped fiber laser at 2 μm ," *Laser Phys. Lett.*, vol. 10, no. 5, p. 055103, May 2013.

- [8] C. Liu, C. Ye, Z. Luo, H. Cheng, D. Wu, Y. Zheng, Z. Liu, and B. Qu, "High-energy passively Q-switched 2 μm Tm³⁺-doped double-clad fiber laser using graphene oxide-deposited fiber taper," *Opt. Exp.*, vol. 21, no. 1, pp. 204–209, Jan. 2013.
- [9] T. Hakulinen and O. G. Okhotnikov, "8 ns fiber laser Q switched by the resonant saturable absorber mirror," *Opt. Lett.*, vol. 32, no. 18, pp. 2677–2679, Sep. 2007.
- [10] J. Liu, J. Xu, and P. Wang, "Graphene-based passively Q-switched 2 μm thulium-doped fiber laser," *Opt. Commun.*, vol. 285, no. 24, pp. 5319–5322, Nov. 2012.
- [11] O. Okhotnikov, A. Grudinin, and M. Pessa, "Ultra-fast fiber laser systems based on SESAM technology," *New J. Phys.*, vol. 6, p. 177, Nov. 2004.
- [12] P. Agrawal, *Application of Non-Linear Fiber Optics*. Boston, MA, USA: Academic, 2007.
- [13] H. Ahmad, A. Z. Zulkifli, K. Thambiratnam, and S. W. Harun, "Q-switched Zr-EDF laser using single-walled CNT/PEO polymer composite as a saturable absorber," *Opt. Mater.*, vol. 35, no. 3, pp. 347–352, Jan. 2013.
- [14] T. Hasan, Z. Sun, F. Wang, F. Bonaccorso, P. H. Tan, A. G. Rozhin, and A. C. Ferrari, "Nanotube–polymer composites for ultrafast photonics," *Adv. Mater.*, vol. 21, no. 38/39, pp. 3874–3899, Oct. 2009.
- [15] Z. Sun, D. Popa, T. Hasan, F. Torrisi, F. Wang, E. J. R. Kelleher, J. C. Travers, V. Nicolosi, and A. C. Ferrari, "A stable, wideband tunable, near transform-limited, graphene-mode-locked, ultrafast laser," *Nano Res.*, vol. 3, no. 9, pp. 653–660, Sep. 2010.
- [16] Z. Jun-Qing, W. Yong-Gang, Y. Pei-Guang, R. Shuang-Chen, C. Jian-Qun, D. Ge-Guo, Y. Yong-Qin, Z. Ge-Lin, W. Hui-Feng, L. Jie, and Y. H. Tsang, "Graphene-oxide-based Q-switched fiber laser with stable five-wavelength operation," *Chin. Phys. Lett.*, vol. 29, no. 11, p. 114 206, Nov. 2012.
- [17] K. Kashiwagi, S. Yamashita, and S. Yun, "In-situ monitoring of optical deposition of carbon nanotubes onto fiber end," *Opt. Exp.*, vol. 17, no. 7, pp. 5711–5715, Mar. 2009.
- [18] A. Martinez, K. Fuse, B. Xu, and S. Yamashita, "Optical deposition of graphene and carbon nanotubes in a fiber ferrule for passive mode-locked lasing," *Opt. Exp.*, vol. 18, no. 22, pp. 23 054–23 061, Oct. 2010.
- [19] H. Ahmad, F. D. Muhammad, M. Z. Zulkifli, and S. W. Harun, "Graphene-oxide-based saturable absorber for all-fiber Q-switching with a simple optical deposition technique," *IEEE Photon. J.*, vol. 4, no. 6, pp. 2205–2213, Dec. 2012.
- [20] R. Paschotta, R. Häring, E. Gini, H. Melchior, and U. Keller, "Passively Q-switched 0.1-mJ fiber laser system at 1.53 μm ," *Opt. Lett.*, vol. 24, no. 6, pp. 388–390, Mar. 1999.
- [21] G. Sobon, J. Sotor, J. Jagiello, R. Kozinski, M. Zdrojek, M. Holdynski, P. Paletko, J. Boguslawski, L. Lipinska, and K. Abramski, "Graphene oxide vs. reduced graphene oxide as saturable absorbers for Er-doped passively mode-locked fiber laser," *Opt. Exp.*, vol. 20, no. 17, pp. 19 463–19 473, Aug. 2012.
- [22] S. Stankovich, D. A. Dikin, R. D. Piner, K. A. Kohlhaas, A. Kleinhammes, Y. Jia, Y. Wu, S. Binh, T. Nguyen, and R. S. Ruoff, "Synthesis of graphene-based nanosheets via chemical reduction of exfoliated graphite oxide," *Carbon*, vol. 45, no. 7, pp. 1558–1565, Jun. 2007.
- [23] J. Xu, J. Liu, S. Wu, Q.-H. Yang, and P. Wang, "Graphene oxide mode-locked femtosecond erbium-doped fiber lasers," *Opt. Exp.*, vol. 20, no. 14, pp. 15 474–15 480, Jul. 2012.
- [24] M. S. Dresselhaus, A. Jorio, M. Hofmann, G. Dresselhaus, and R. Saito, "Perspectives on carbon nanotubes and graphene Raman spectroscopy," *Nano Lett.*, vol. 10, no. 3, pp. 751–758, Mar. 2010.
- [25] S. W. Harun, M. A. Ismail, F. Ahmad, M. F. Ismail, R. M. Nor, N. R. Zulkepely, and H. Ahmad, "A Q-switched Erbium-doped fiber laser with a carbon nanotube based saturable absorber," *Chin. Phys. Lett.*, vol. 29, no. 11, p. 114 202, Nov. 2012.
- [26] S. J. Tan, S. W. Harun, N. M. Ali, M. A. Ismail, and H. Ahmad, "A multi-wavelength Brillouin Erbium fiber laser with double Brillouin frequency spacing and Q-switching characteristics," *IEEE J. Quantum Electron.*, vol. 49, no. 7, pp. 595–598, Jul. 2013.